

1 The architecture of multifunctional ecological networks

2 Sandra Hervías-Parejo^{1,3*}, Mar Cuevas-Blanco^{2*}, Lucas Lacasa^{2,+}, Anna Traveset¹,
3 Isabel Donoso¹, Ruben Heleno³, Manuel Nogales⁴, Susana Rodríguez-Echeverría³,
4 Carlos Melián^{2,5,6} & Victor M. Eguíluz^{2,7,8,+}

5 ¹Mediterranean Institute for Advanced Studies (IMEDEA, CSIC-UIB), Esporles, Mallorca, Illes Balears (Spain)

6 ²Institute for Cross-Disciplinary Physics and Complex Systems (IFISC, CSIC-UIB), Palma de Mallorca, Illes
7 Balears (Spain)

8 ³Centre for Functional Ecology (CFE), TERRA Associate Laboratory, Department of Life Sciences, University
9 of Coimbra, Coimbra (Portugal)

10 ⁴Institute of Natural Products and Agrobiology (IPNA-CSIC), La Laguna, Tenerife, Canary Islands (Spain)

11 ⁵Department of Fish Ecology and Evolution, Eawag Centre of Ecology, Evolution and Biogeochemistry,
12 Dübendorf (Switzerland)

13 ⁶Institute of Ecology and Evolution, Aquatic Ecology, University of Bern, Bern (Switzerland)

14 ⁷Basque Centre for Climate Change (BC3), Scientific Campus of the University of the Basque Country, 48940
15 Leioa (Spain)

16 ⁸IKERBASQUE, Basque Foundation for Science, Bilbao (Spain)

17

18 * *SHP and MCB are both first authors*

19 + *LL and VME are both corresponding authors*

20 Abstract

21 Understanding how biotic interactions affect ecosystem functioning has been a research priority in
22 natural sciences due to their critical role in bolstering ecological resilience¹⁻³. Yet, traditional
23 assessment of ecological complexity typically focus on species-species effective interactions that
24 mediate a particular function (e.g. pollination⁴ or seed dispersal⁵), overlooking the synergistic effect of
25 multiple functions that further underpin species-function and function-function interactions in
26 multifunctional ecosystems. At the same time, while ecological network theory holds a potential to

27 quantify the relationship between biodiversity and ecosystem multifunctionality^{6,7}, its connection has
28 been done mainly conceptually, due to challenges measuring different interactions and establishing
29 their relevance across multiple niche dimensions^{8,9}. Such lack of quantitative studies therefore limits
30 our ability to determine which species and interactions are important to maintain the multiple
31 functions of ecosystems¹⁰. Here we develop a framework –derived from a resource-consumer-function
32 tensor analysis- that bridges these gaps by framing biodiversity-ecosystem multifunctionality in terms
33 of multilayer ecological network theory. Its application to recently collected ecological data --
34 reporting weighted interactions between plants, animals and fungi across multiple function types--
35 allows to (i) unveil and quantify the existence of both (multi-functional) keystone species and a dual
36 function kestoneness pattern, and (ii) project plants and functions into a similarity space where clear
37 clusters emerge and the importance of weak links is manifested. This dual insight from species and
38 functional perspectives will better guide conservation efforts to reduce biodiversity loss.

39 **Main**

40 All species are permanently involved in a myriad of entangled interactions with other coexisting
41 species¹¹⁻¹³, playing multiple and simultaneous ecological roles that together define the multiple
42 dimensions of their Eltonian niche^{14,15}. In a nutshell, ecosystems are inherently multidimensional
43 complex systems, and different types of collective effects throughout the complexity hierarchy¹⁶ are
44 therefore expected to emerge, including not only effective species-species interactions but also^{11,12}:
45 species-function interactions (e.g. a herbivore interfering pollination, plant species participating in
46 various functions in heterogeneous ways) and effective function-function (e.g. an animal pollinating
47 and dispersing the same plant species) ones. Thus, any representation aiming to capture the
48 relationship between biodiversity and ecosystem multifunctionality^{6,7} requires incorporating such
49 complexity in a meaningful way, i.e. it needs to enrich biodiversity-ecosystem multifunctionality¹⁰
50 patterns by accounting for species-rich interactions and functions^{17,18}. From a modelling perspective,
51 while traditional mathematical frameworks such as network theory have proven useful to gain insights
52 on, for instance, extinction cascades^{19,20}, there is a need to embrace more sophisticated ones -e.g.

53 multilayer networks²¹⁻²³- in order to naturally incorporate different types of interactions²⁴ (both direct
54 and indirect) into a unique modelling framework. At the same time, accessing the necessary fine-
55 grained empirical observations of species interactions is inherently a difficult task²⁵, often resulting in
56 incomplete observations or indirectly-inferred^{26,27} data. In addition, multilayer modelling requires
57 stringent standardised measurements of species' importance in each function (i.e. using the same
58 currency to quantify different types of interactions), thereby hampering advances in the field.
59 Integrating several ecological functions, thus, represents both a necessity and a challenge²⁸ given the
60 difficulties imposed by data collection and standardisation, and their subsequent translation into
61 appropriate modelling paradigms. As a result, there is a lack of quantitative studies connecting
62 biodiversity-ecosystem multifunctionality to ecological networks^{8,29}.

63 Here we take the first steps to bridge this gap, both from a theoretical and experimental viewpoints.
64 Our modelling approach is inspired by the consumer-resource paradigm^{30,31}, whereby plants are seen
65 as “resources”, and “consumers” encapsulate different types of animals or fungi involved in both
66 mutualistic and antagonistic interactions (note, however, that the methodology and analysis can be
67 generally extended to other systems where a consumer-resource paradigm exists, such as economic
68 systems³²). By extending multiple consumer-resource interactions to many functions, the biodiversity-
69 ecosystem multifunctionality relationship can therefore be analysed not only from a multiple
70 interaction but also from a multiple function perspective. Then, by leveraging the relative simplicity
71 of a small island ecosystem -Na Redona, in the Balearic Islands (W Mediterranean Sea)-, we apply
72 such a framework to unveil the multifunctional architecture of an ecological system reconstructed via
73 fieldwork data encompassing a total of 1537 weighted interactions between plants, animals and fungi
74 across six ecological functions (layers). Our common species in all six layers are plants, which
75 interact with pollinators, herbivores, seed dispersers, and three types of (pathogenic, saprotrophic and
76 symbiotic) fungi.

77 Operationally, we will first proceed to integrate the multiple dimensions of ecological
78 interactions into a Resource-Consumer-Function tensor (hereafter RCF). The RCF can be visualised
79 as a (multipartite) multilayer weighted network. The architecture of MultiFunctional Ecological

80 Networks (hereafter MFEN) can be decoded from the RCF itself by suitably contracting the consumer
81 index and yielding a resource-function matrix or map. We will show that the representation of the
82 MFEN in the Na Redona system displays a nested pattern³³. As MFEN studies the architecture of
83 species-to-function interactions, interpreting such pattern necessarily leads to the existence of both
84 (multifunctional) keystone species and, notably, also 'function kestoneness', a new concept we coin
85 and discuss here. As a matter of fact, while all ecological functions are important, one can indeed ask
86 whether their roles as ecosystem assemblers are similar or not, and how interactions and functions
87 connect each other, to form a keystone interaction-function core containing the most critical functions
88 for ecosystem functioning. We propose that this perspective aligns with approaching the ecosystem
89 through a function-centric lens, rather than a traditional phytocentric one. Indeed, just as keystone
90 species encode, among other properties, robustness (i.e. the ability to maintain performance in the
91 face of perturbations) and resilience³⁴, the response of the ecosystem to some disturbances may also
92 occur in the functional dimension. For instance, non-native herbivores can disrupt chemically-
93 mediated interactions between plants and herbivores, pollinators, predators, and parasites that respond
94 to herbivore-induced plant volatile cues³⁵. Because there is a wide variety of interactions involving
95 native organisms that a single non-native could potentially impact, the challenge lies in determining
96 which functions should be prioritised. Therefore, defining and identifying key ecological *functional*
97 *cores* -critical for proper ecosystem development and balance- and studying the robustness and
98 adaptation of these functional cores to disturbances can be crucial to understanding ecosystem
99 functioning and resilience³⁶.

100 Below, we illustrate how distinct methods applied to the original RCF tensor directly enable us to
101 address and quantify a wide range of significant ecological questions within a unified methodological
102 framework. These inquiries encompass determining multifunctional species kestoneness, the dual
103 challenge of function kestoneness, and keystone functional cores to assess ecosystem clustering and
104 robustness against perturbations of species or functions, and even establishing a resource-function
105 mapping. Each of these questions indeed mirror different facets of the polyhedral structure of the
106 ecosystem (see **Fig. 1** for an illustration of each step of the framework). Application of the proposed

107 framework to data gathered in Na Redona islet unveils an intertwined keystone hierarchy both in
108 the species and function dimensions that overall provide a better understanding of the complex
109 structure of ecosystems.

110

111 **Complete data representation: the Resource-Consumer-Function tensor (RCF).** The
112 precise span of dimensions is driven by the extent of our data (see Methods), which includes direct
113 observation of 16 plant species, 629 fungal ASV (i.e. amplicon sequence variants) and 46 animal
114 species, interacting across six fundamentally different ecological functions (pollination, herbivory,
115 seed-dispersal, decomposition, nutrient uptake, fungal pathogenicity). The complete relational dataset
116 is thus formalised in terms of a rank-3 tensor $\mathbf{F} = \{ f_{ix}^\alpha \}$ that we call the RCF. Interpreting the
117 architecture of this tensor as a network²¹, we see that RCF displays two groups of nodes: resource
118 nodes (plant species, denoted by Latin letters i, j), and consumer nodes (different animal and fungi
119 species, denoted by the Latin letter x). By construction, such network is *multipartite*, since
120 interactions (links) take place between groups, but no direct intragroup is directly recorded.
121 Furthermore, links characterise different types of interactions, and, therefore, the network is naturally
122 a *multilayer* one²², where each layer represents the wiring architecture according to a concrete
123 function (functions are denoted by Greek letters α, β). Finally, such network is *weighted*: for each
124 layer α , data allows us to calibrate the strength of the interaction between a resource node (plant
125 species i) and a consumer node (animal/fungi species x), resulting in the link weight f_{ix}^α ($0 \leq f_{ix}^\alpha \leq$
126 1, see Methods).

127 The RCF can be effectively visualised as a multipartite edge-coloured weighted network (see
128 **Fig. 2**, after having processed the layout via the Infomap community detection algorithm; details
129 provided in Methods), revealing that consumers are often centred around a single plant species,
130 forming clusters (see, however, the cluster consisting of *Lavatera maritima* and *Geranium molle*).
131 Interestingly, cross-cluster links are also present, depicting that the ecosystem is formed by many
132 clusters connected via an animal/fungi consortium. For alternative visualisations of the RCF tensor,
133 see Extended Data Figure **EDF1**.

134

135 **The Multifunctional Ecological Network (MFEN).** To quantify the relationship between
136 species and ecological functions the system embodies, we ‘contract’ the consumer indices into the
137 RCF tensor, thereby building a *resource-function matrix*, which is the weighted adjacency matrix of
138 the (bipartite) Multifunctional Ecological Network (MFEN). The weights of this bipartite network P_i^α
139 are called *participation strengths* and account for the probability that i participates in function α . To
140 These are estimated from the empirical values of f_{ix}^α , and making the parsimonious assumption of no
141 correlation between consumers, which yields $P_i^\alpha = 1 - \prod_x (1 - f_{ix}^\alpha)$ (see Methods for the derivation and
142 **Fig. 3a** for an illustration). This choice for computing P_i^α is parsimonious and can be refined to
143 incorporate correlations (e.g. via the co-visitation patterns of two or more pollinator species) if
144 empirical evidence of such correlation kernels is eventually available (e.g. via phylogenetic, trait
145 similarity or field).

146 The MFEN is thus given by the matrix $\mathbf{P} = \{P_i^\alpha\}$, where i ranges across plant species and α ranges
147 across functions^a. The resulting \mathbf{P} obtained with our empirical data from Na Redona is presented in
148 **Fig. 3b** (a visualisation of the bipartite network is also provided in **Fig. 3c**). \mathbf{P} clearly displays (see
149 below) a stylised nested structure, as commonly found in, for example, mutualistic interaction
150 networks, world trade, inter-organisational relations, and others³³, although in this case such pattern
151 notably emerges in a species-to-function setting.

152 Observing such a nested pattern firstly indicates that the participation of plant species throughout
153 different ecological functions is heterogeneous. To classify species as ecological function-generalists
154 or function-specialists, it is crucial to consider both the number of functions in which they participate,
155 and the strength of their participation³⁷. For instance, *Withania frutescens* and *Lavatera maritima*
156 participated in all six functions with an average probability of 0.6 or greater, indicating they act as
157 generalist species. In contrast, others such as *Chenopodium murale* and *Heliotropium sp.* emerge as
158 more “function-specialists”, participating in four out of the six functions with lower average

^aNote the slight abuse of notation in calling \mathbf{P} a matrix instead of a rank-2 tensor: throughout this work, for simplicity, we shall call tensor only rank-3 tensors –as the RCF–, whereas all rank-2 tensors are called (adjacency) matrices, regardless the number of covariant and contravariant indices.

159 probabilities (0.3 or less) (see **Fig. 3e** for a simple preliminary quantification). The emergence of such
160 hierarchy suggests the existence of *multifunctional keystone plant species*, as we will fully develop
161 and quantify below.

162 Second, the non-trivial nested pattern also suggests the existence of functions that are ‘plant-
163 generalist’ -meaning they are participated by many plant species with systematic high participation
164 strength-. This is for instance the case of decomposition –via saprotrophic fungi-, with an average
165 participation of 0.7 by all plant species. This can then be compared to other functions, which are
166 participated by fewer plant species with weaker strength, such as seed-dispersal -with an average
167 participation of 0.2 by 9 of the 16 species- (**Fig. 3d** provides a preliminary quantification).
168 Interestingly, finding a heterogeneous degree of participation opens up the question of whether and
169 how robust an ecosystem is with respect to perturbations to functions (instead of species as commonly
170 assumed), and overall naturally leads to formulating the novel concept of *function kestoneness*, that
171 we will also fully develop and quantify later.

172

173 **Phytocentric embedding: function-function networks and Multifunctional plant species**

174 **kestoneness.** We now dive deeper into the multifunctional species kestoneness initially identified
175 in **Fig. 3e**, and into the role that plant species play as ecosystem assemblers (i.e. the phytocentric
176 perspective). To this aim, we proceed to project MFEN into the function class and thus extract a
177 function-function effective interaction network with $N=6$ nodes and weighted adjacency matrix $\Phi =$
178 $\mathbf{P}^T \mathbf{P}$ (superindex T denotes matrix transposition) that leverages how species connect –actually,
179 broker– functions in the ecosystem. Mathematically, Φ allows for several equivalent interpretations.
180 First, the elements $\Phi^{\alpha\beta} = \sum_i P^{\alpha}_i P^{\beta}_i$ enumerate the effective paths (passing via a resource-species)
181 connecting two functions α and β , and by weighting such paths, effectively compute the expected
182 number of paths connecting α and β . This is therefore based on the number of plant species that
183 simultaneously participate in both functions α and β , and hence quantifies the role of plant species as
184 function assemblers. Second, interpreting the different participation strengths as function features, Φ
185 adopts the mathematical form of a correlation matrix, i.e. a similarity-based matrix (see Methods), and

186 quantifies how similar functions are to each other based on their participation strength pattern across
187 plant species, i.e., in a plant-feature embedding. See **Fig. 4a** for a visualisation of Φ of the Na Redona
188 dataset, showing that edge weights are indeed heterogeneous, indicating that plants impact functions
189 assembly/homophily in a non-trivial way.

190 First, we can explore how functions are intertwined at different resolution scales in such plant
191 embedding by sequentially pruning edges in Φ and monitoring the size of the largest connected
192 component (LCC): e.g. if pruning a low-weight link had the immediate effect of separating the
193 network into two clusters of similar size, this would mean functions belonging to each cluster would
194 play similar (intra-cluster) ecological roles, and dissimilar roles for each cluster. Conversely, if
195 pruning low-weight links did not have a noticeable effect on the size of the LCC, this would mean that
196 all functions have similar ecological roles. Now, edge pruning can be performed in several ways,
197 where an obvious choice is to sequentially remove edges in ascending link weight, allowing us to
198 evaluate the role of so-called *weak ties*³⁸ as potential assemblers. Conversely, one can also remove
199 edges with higher weight first (see Methods). In **Fig. 4b** we plot how the (normalised) size of the
200 LCC, $S(m)/n$, of the pruned Φ as pruning is performed, for both pruning strategies. Results show that
201 at first order the function-function network is “robust” against plant species extinctions -as it remains
202 mostly unaltered until over 50% of the edges have been pruned-, i.e. functions perform similar roles in
203 the plant-mediated similarity space. Interestingly, we also find that edges with lower weight – pairs of
204 functions which are more dissimilar in this plant-mediated projection, i.e. weak ties– tend to be
205 slightly more critical for the network assembly, as the net difference in Area Under the Curve (AUC)
206 between both pruning strategies is about +9%. This result seems in agreement with the theory of weak
207 ties³⁸ -originally put forward in the context of social systems, and studied theoretically in models of
208 correlated networks³⁹-, where less homophilic ties e.g. tend to be more relevant for network assembly.
209 In order to further inspect the clustered structure of functions in this plant-feature embedding, we also
210 performed a hierarchical clustering of the system, by interpreting the inverse $1/\Phi^{\alpha\beta}$ as the entries of a
211 dissimilarity matrix. Results (**EDF2**) show that functions cluster together forming an intertwined core,
212 with seed dispersal (and to some extent, fungal pathogenicity) being more peripheral.

213 Second, we already noted that each term $P^{\alpha_i}P^{\beta_i}$ in the summation of $\Phi^{\alpha\beta}$ encodes the contribution
214 of each specific plant species i to the connection (similarity) between functions α and β . Thus, the
215 specific role of species i as a broker of functions can subsequently be disentangled from Φ by
216 conditioning Φ only on a particular plant species i , and then appropriately visualised as a weighted
217 (hexagonal-shaped) 6-node network $\Phi|_i$, where (i) each node α represents a different function and is
218 enriched with a node weight P^{α_i} (according to the likelihood that the plant species i participates in
219 that function), (ii) links between pairs of functions α and β denote that plant species i participates in
220 both functions and the link weight $\Phi^{\alpha\beta}|_i := P^{\alpha_i}P^{\beta_i}$ quantifies that contribution^b: see **Fig. 4c** for
221 some examples and **EDF3** for the complete set of networks $\{\Phi|_i\}$. The *metadata* (properly
222 normalised sets of nodes and edges' weights) of $\Phi|_i$ informs the (multifunctional) participation
223 pattern of each plant species i in the whole ecosystem. Thus we use of such metadata to rank plant
224 species' multifunctional keystone ness. Since in this work we have a total of 6 observed functions, we
225 associate to each plant species i a 6-dimensional vector (appropriately normalised), where each entry
226 of the vector is $\sum_{\beta} P^{\alpha_i} P^{\beta_i} / \sum_j \sum_{\beta} P^{\alpha_j} P^{\beta_j}$: a *multifunction participation index* that quantifies the
227 contribution to keystone ness of i via a particular function α (see Methods). The L₁-norm of this vector
228 thus provides the ranking ordering (see **Fig. 4d**). For better visualisation, in this figure we colour-code
229 each element of the vector according to the function it corresponds to and plot the magnitude of each
230 element as a coloured-segment of different length (the norm of the vector is thus the concatenation of
231 line segments). This ranking summarises the role played by each plant species in assembling the
232 ecosystem as propagated into the dual function-function representation (see also SI and **EDF4** and
233 **EDF5** for complementary metrics). As we can see, some plant species such as *Withania frutescens* or
234 *Lavatera maritima* play a critical role in every function and are thus at the top of the ranking (this
235 agrees with complementary analysis in **EDF7** and **EDF9**). In contrast, some other species such as
236 *Heliotropium sp.* or *Asparagus horridus* play a much weaker role.

^b This is compatible with the interpretation that the probability that a resource i is observed participating in two functions could be obtained from the product of the probabilities, as in **Fig. 3a**. Such no-correlation scenario leads the resulting matrix to be in the universality class of so-called rank-1 networks⁴⁰, and can also be understood under the paradigm of fitness-mediated good-get-richer networks⁴¹ or a particular class of hidden variable network⁴².

237 Finally, it is important to clarify that the (multifunctional) species keystone index above does
238 not correlate significantly with species relative abundance (Pearson $r = 0.31$, p -value = 0.24) or
239 vegetation cover (Pearson $r = 0.47$, p -value = 0.06) (see **EDF6** and Extended Data Table **EDT1** for
240 statistical details), suggesting that such keystone index is neither directly related to potential sampling
241 biases nor is a simple byproduct of species abundance, pointing to a more subtle property, unveiled
242 here through our formalism.

243

244 **Dual Function-centric embedding: plant-plant networks and (multispecies) function
245 keystone index.** The dual concept of *function keystone index* can be explored following similar
246 mathematical manipulations as in the phytocentric perspective: initially starting from MFEN, we
247 project now onto the plant class (function-feature embedding) and thus construct a resource-resource
248 (i.e. plant-plant) effective interaction network with $N=16$ nodes and weighted adjacency matrix $\mathbf{\Pi} =$
249 $\mathbf{P}\mathbf{P}^T$, that leverages how *functions* broker the interaction between resources. Its elements $\Pi_{ij} = \sum_a P^a_i P^a_j$
250 quantify the expected number of shared functions by two plant species, or alternatively how similar
251 two plant species are in a function-feature embedding, see **Fig. 5a** where we again find that edge
252 weights are heterogeneous. We then proceed to explore how functions act as plant species assemblers
253 by performing a pruning analysis of $\mathbf{\Pi}$. Results (**Fig. 5b**) suggest that plant species are more clustered:
254 the pruning strategy of removing the edges with higher weight first (i.e. removing the links for the
255 pairs of plants which show higher similarity in function-centric projection) leaves the plant-plant
256 network unaltered until about 70% of the edges have been pruned, but conversely, the network
257 smoothly dismantles after removal of 35% of the edges with lower weight. These findings reaffirm
258 the significance of *weak ties* in this ecological context. In other words, plant-plant interactions that on
259 average have a lower weight (i.e. are overall mediated by fewer functions or are observed less
260 frequently or with different patterns, i.e. more dissimilar plant species) have a more critical role as
261 plant-plant assemblers. Moreover, the net difference of AUC between both pruning strategies is about
262 +16%, almost twice as large as that found for the function-function network, overall suggesting that
263 functions have a more hierarchical role than plants. Finally, AUC for the plant-plant network

264 descending-order pruning analysis (0.93) is greater than the respective AUC (0.84) for the function-
265 function network. This implies that comparatively speaking, the plant-plant network is more cohesive
266 (i.e. displaying more function-based similarity) than the other way around, i.e. functions assemble
267 plants slightly more than the other way around.

268 We also analysed how plants cluster together at different resolution scales in this function-feature
269 embedding by computing a hierarchical clustering on a dissimilarity matrix whose entries are $1/\Pi_{ij}$,
270 see **EDF7**. Interestingly, clusters of plants to reflect the multifunctional species keystone found in
271 **Fig 4.d.**

272 Finally, to evaluate and rank the role of each specific function as an ecosystem assembler, we
273 replicate the analysis performed before and proceed to disaggregate Π by conditioning on each
274 function, in order to extract 6 different plant-plant networks (one per function α) with weighted
275 adjacency matrices $\Pi|\alpha$ with elements $\Pi_{ij}|\alpha = P_i|\alpha P_j|\alpha$ (see **Fig. 5c** for some examples^c and **EDF8** for
276 the complete set $\{\Pi|\alpha\}$). The metadata of $\Pi|\alpha$ provides the plant participation of each function α and
277 a ranking of *(multispecies) function keystone* can be derived (**Fig. 5d**). This ranking certifies the
278 heterogeneity of roles and impacts of the different functions (to be compared with **EDF2**).

279

280 **Discussion.** Our proposed RCF/MFEN framework offers a comprehensive and mathematically
281 sound approach to unveil the complex architecture of multifunctional ecosystems. Let us first discuss
282 and interpret in some detail the findings of such analysis as applied to the Na Redona dataset.

283 Results of the phytocentric perspective indicate that plant species contribute hierarchically to multiple
284 functions, i.e. they multitask⁴³. Interestingly, the first six species in the keystone hierarchy, i.e.
285 those with the highest multitasking indices, are all woody shrubs. The rest, except for *Ephedra*
286 *fragilis*, are all herbaceous. Herbs such as *C. murale* and *Heliotropium* sp. play a minor role in linking
287 the overall network, which does not mean they are not important for particular ecological functions.
288 The finding that woody shrubs are those more strongly involved in different functions might be

^c The conditioned plant-plant networks are again in the universality class of rank-1 networks⁴⁰ and can be interpreted as fitness-based or hidden variable networks^{41,42}.

289 attributed to the longer lifespan of such species compared to herbs, which allows them to link to a
290 wider array of species in each type of interaction. However, more in-depth studies are needed to
291 unveil the exact mechanism of such multitasking. Interactions between plants and fungi (especially
292 saprotrophic and pathogenic fungi) were found to play the most important role in assembling the
293 multitrophic network. Microbial decomposers, together with plants and herbivorous insects, are also
294 important drivers of ecosystem functioning in grasslands, where a positive association has been
295 documented between richness or abundance and multiple ecosystem services⁴⁴.

296 Results on the function-centric perspective suggest that saprophytic interactions (decomposition)
297 exhibit a disproportionate prevalence: this agrees with a relatively recent shift in the interest and
298 relevance of underground –in contrast to above-ground- ecological interactions. In any case, the
299 pattern remains hierarchical (some plants dominate in one function while others play a dominant role
300 in another or several functions), as quantified by our measures of multispecies function keystone ness.

301 The finding that weaker function-function and plant-plant effective interactions (lower similarity
302 ones) tend to play an important role in assembling the multifunctional ecosystem in these embeddings
303 is reminiscent of the behaviours reported in social networks^{38,46}, where less frequently used
304 interactions or less homophilic ones are those which tend to be information brokers, and the overall
305 system tends to be more fragile against perturbations of these weaker links³⁹.

306 Finally, it is worth noting that our whole framework is in principle metric-agnostic, i.e. while we used
307 some specific quantification metrics, others alternatives are also possible⁴⁵ (see SI for complementary
308 metrics).

309 Now, it is important to acknowledge that there are certain limitations to our analysis and
310 methodology, mainly associated with the unavoidable specificities of data collected in the Na Redona
311 islet. First, the particular contraction method we used of the original tensor is based on the fact that in
312 each layer, the interactions are bipartite; that is, there are no direct interactions between plants or
313 between animals/fungi. Consequently, incorporating competition between plants and/or animals/fungi
314 might eventually require some refinement of the framework. Second, while multifunctional, our
315 collected data is eminently phytocentric, instead of zoocentric. If newer data allows us to account for

316 purely zoocentric observations (ideally mixed plant-zoo-centric observations), retaining the complete
317 RCF tensor would be convenient instead of contracting it. Third, since field observations were
318 focused primarily on plants, we lack specific information, such as the trajectory of insect pollinators.
319 Consequently, we cannot directly quantify the probability that a plant is included in the diet of a
320 particular insect pollinator species. In this case, the parsimonious approach is to assume
321 independence, and this is the base of our derivations. However, the contribution of a plant species to a
322 function is typically mediated by the participation of several animal/fungal species, and the existence
323 of correlations in the behaviour of different species is possible. Take for example, again, pollination.
324 In our calculations we assumed that a universal probability governs whether a specific plant is visited
325 or not. However, we do know that plants may attract specific pollinator species (especially the most
326 specialised ones that have particular flower traits, e.g. long corolla tubes), resulting in a latent
327 correlation kernel. Accordingly, the advent of new data should be used to test the validity of our
328 parsimonious assumption.

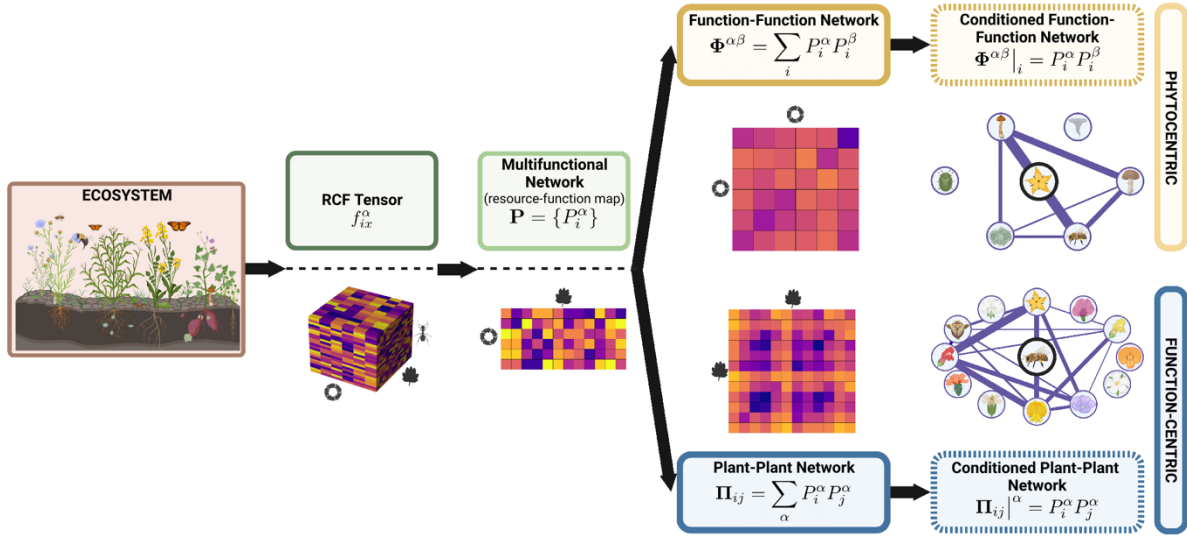
329 We shall now provide some final remarks on our proposed framework. The RCF tensor serves as
330 a powerful tool for capturing and quantifying the multidimensional nature of ecosystems. It facilitates
331 data standardisation by integrating the multifunctional dimension into a resource-consumer(*-function*)
332 paradigm and its contraction into a MFEN leads to an effective resource-function mapping, providing
333 valuable insights into the interplay between the phytocentric and function-centric perspectives.
334 Indeed, this framework is conceptually general and can be easily extended to characterise such
335 interplay in other complex systems. For instance, it can be applied to genetics, where our resource-
336 function mapping resembles a classical genotype-phenotype map⁴⁸, illustrating how genes interact to
337 give rise to phenotypes in various animals. Similarly, in economic systems, this interplay can shed
338 light on how goods are traded among countries across different economic sectors⁴⁹. The MFEN (and
339 its projections) unveils the duality of plant species and interaction functions (phyto vs function-centric
340 perspectives), where the concept of multifunctional species keystonehood and the dual concept of
341 (multispecies) function keystonehood naturally emerge as two (interconnected) sides of the same coin.
342 The former refers to species that play key roles to maintain a multifunctional system –with impact on

343 e.g. network stability⁴³-. In contrast, the latter refers to the different roles functions play in keeping
344 species coexistence in an ecosystem. Both concepts are indeed intertwined, feeding back into each
345 other. For instance, in the context of climate change, it is not uncommon to witness drastic and
346 sustained temperature increases over large geographic regions. If such exogenous perturbations
347 induce, e.g. phenological mismatches between flowering plants and insect pollinator visits, then the
348 complete pollination function might be threatened before any of the species are themselves
349 threatened⁵⁰, i.e. perturbation takes place initially in the function dimension. It can then propagate
350 with potential cascading effects for both species and other functions, as described in the resource-
351 function map. Conversely, the decline or extinction of a seed disperser (animal species dimension)
352 may trigger declines or plant extinctions, which in turn cascade to affect species involved in other
353 ecological functions, such as underground fungi⁵¹. Furthermore, the extinction of a keystone plant
354 species can also influence other species' interactions, either by causing interaction rewiring or by
355 modifying interaction strengths⁵². Such cascading effects across interaction types become particularly
356 problematic in double-mutualistic interactions, i.e. when the same animal acts, for example, as
357 pollinator and seed disperser of the same plant species⁵³. Yet, not only the disruption of mutualistic
358 interactions but also of antagonistic interactions could derive functional losses, e.g. the loss of top
359 predators may indirectly affect ecosystem productivity and metabolism⁵⁴. However, few studies still
360 exist on how human activities can alter ecosystem multifunctionality, both directly on ecosystems and
361 indirectly through the loss of multifunctional biodiversity^{6,55}. Moreover, how organisms at different
362 trophic levels interact to influence ecosystem multifunctionality in the presence of multiple concurrent
363 anthropogenic drivers remains largely unexplored^{44,56}. Thus, we hope our framework offers a
364 promising approach for evaluating the relative vulnerability of ecosystem functions to anthropogenic
365 stressors. As we delve deeper into understanding ecosystems, the integration of temporal, spatial, and
366 dynamical features within this framework, coupled with its application to ecological data from other
367 environments, emerge as exciting avenues for future research.

368

369

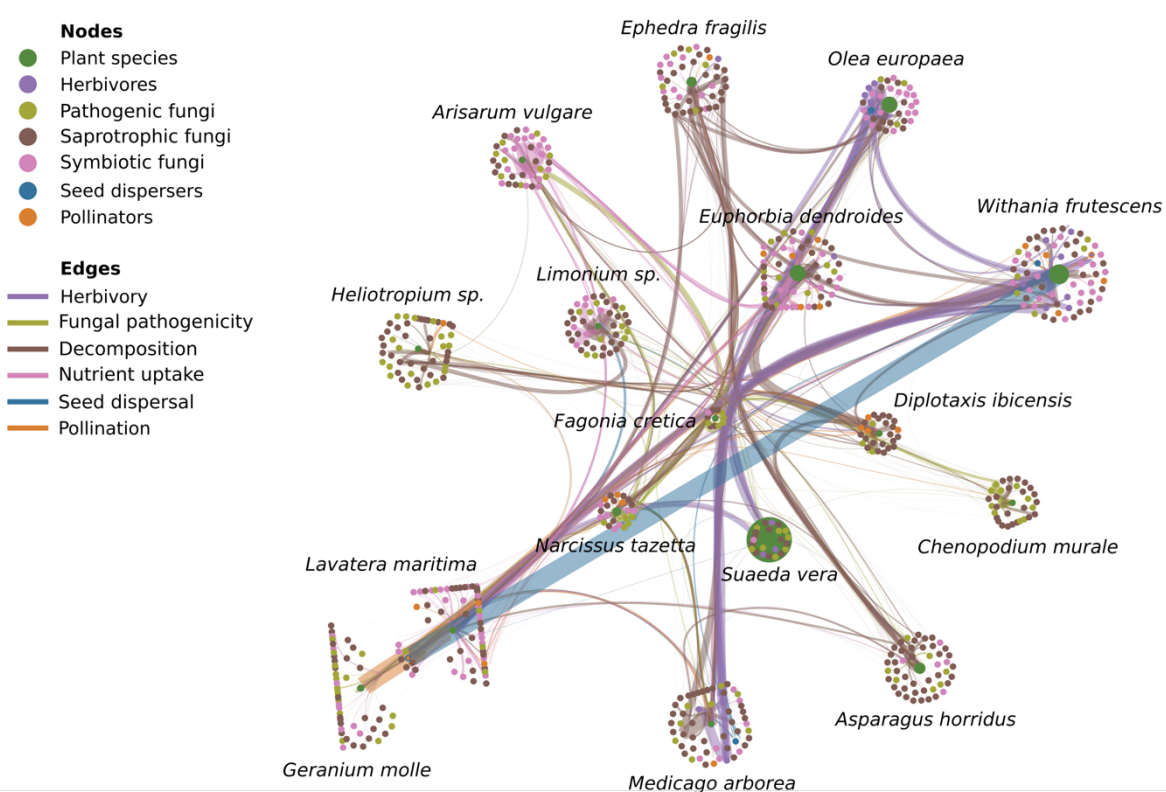
370 **Figures**



371

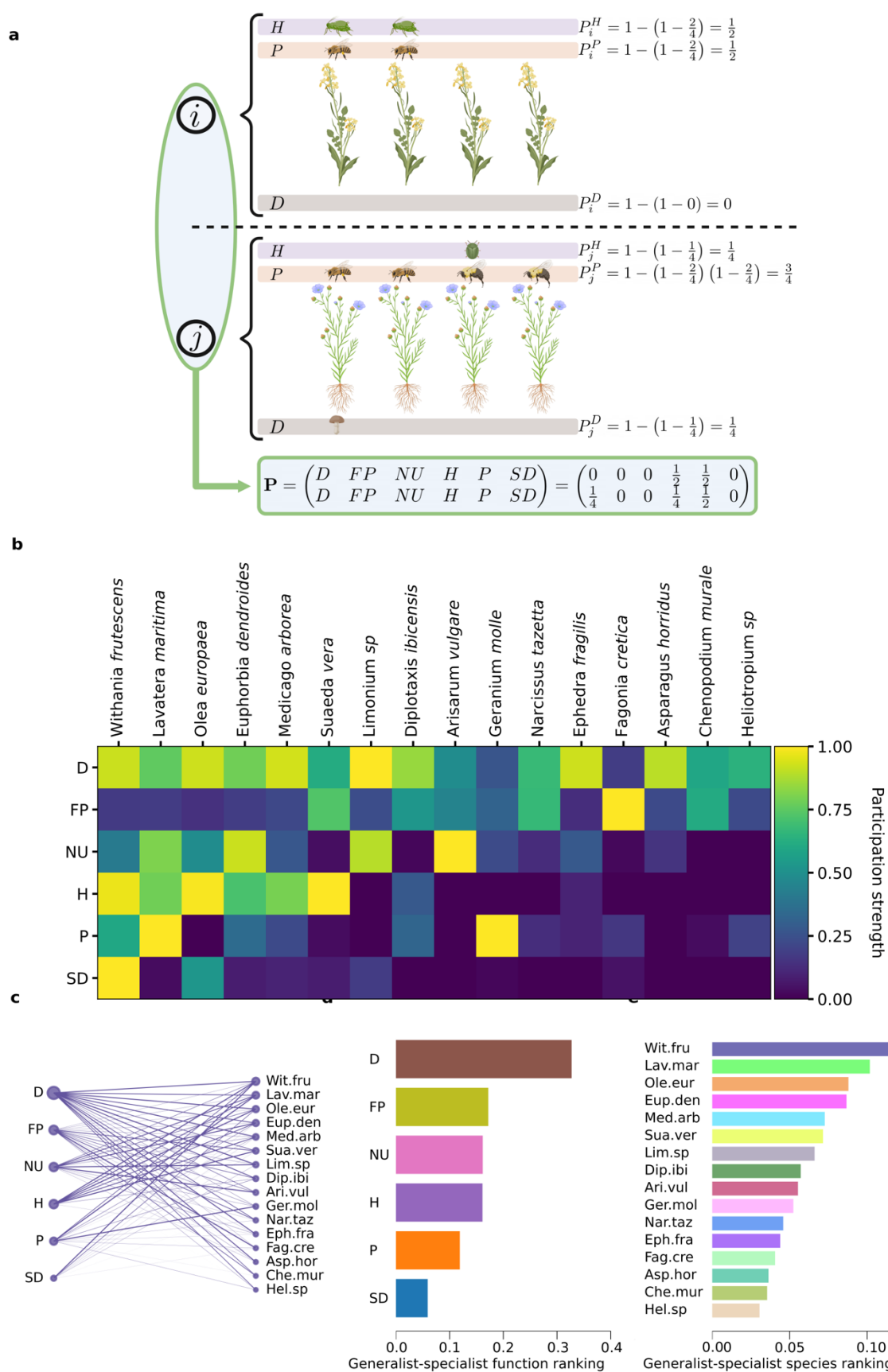
372 **Figure 1. Conceptual framework.** Ecosystems are multidimensional complex systems whose
373 interactions are captured by a rank-3 Resource-Consumer-Function tensor (here, a plant-
374 animal/fungi ecological interaction tensor). Contracting consumers out, we obtain a resource-
375 function matrix or map –the MultiFunctional Ecological Network (MFEN)– that encapsulates how
376 plant species and functions are intertwined in the ecosystem. Further projections of MFEN yield
377 function-function networks that characterise how each plant species participate and intertwine
378 different functions (phytocentric embedding) and plant-plant networks that characterise how each
379 ecological function participates and intertwines different plant species (function-centric embedding).
380

381



382

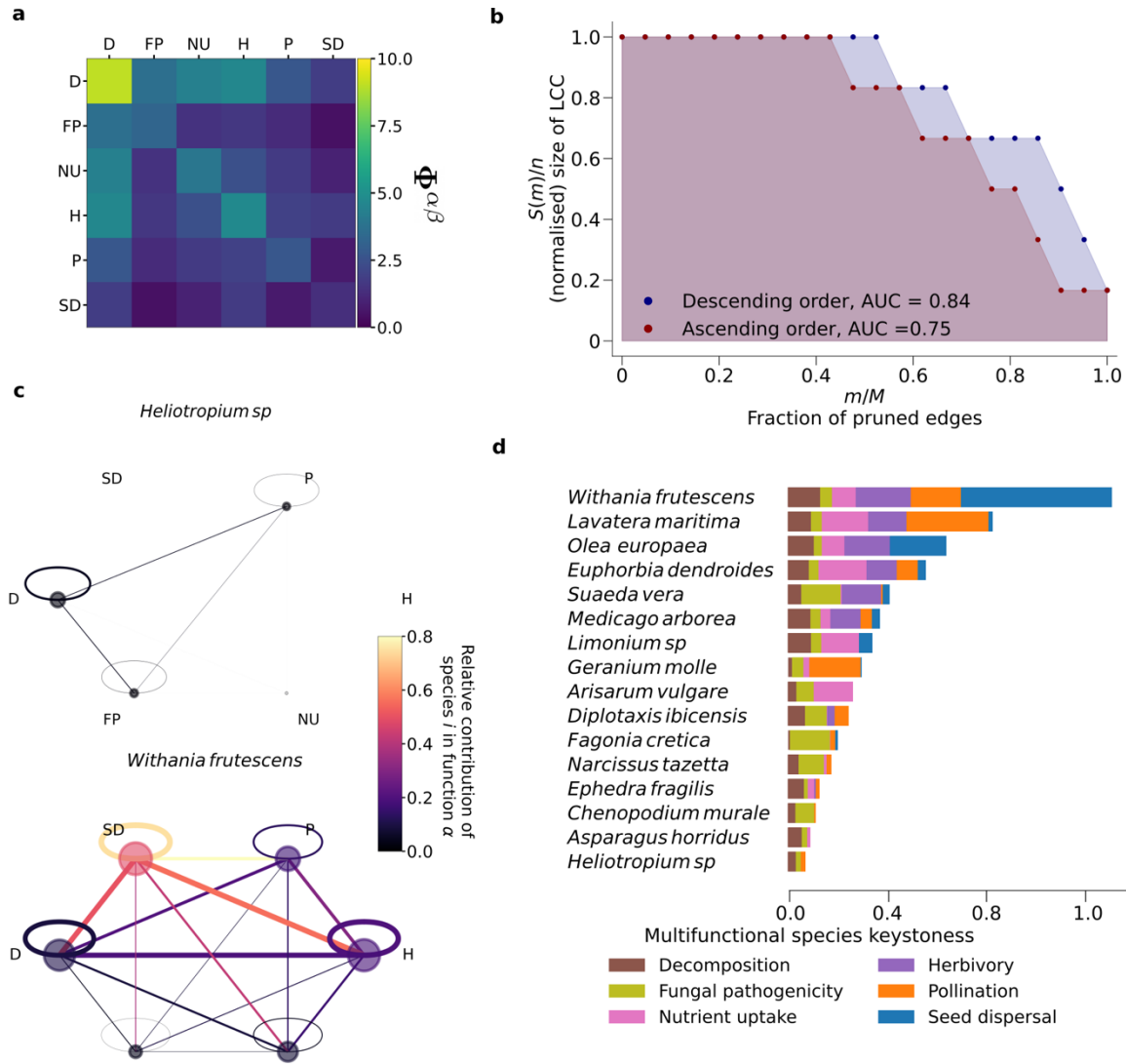
383 **Figure 2. Basic visualisation of the Resource-Consumer-Function tensor (RCF) from the Na**
384 **Redona dataset.** There are 691 nodes (16 plant species and 675 animal/fungus species) interacting
385 via six functions: pollination, herbivory, seed-dispersal, decomposition of plant matter, nutrient
386 uptake (mycorrhizas), and fungal pathogenicity, for a total of 1573 weighted interaction links. Node
387 colours account for plant species (green) and animal/fungus species (colour-coded according to the
388 primary function they are involved in). The sizes of plant-nodes represent their observed abundance
389 in the field (see Methods). Link widths quantify the weight of interaction and link colours denote the
390 functional interaction type. In this suitable layout, species are clustered via Infomap's community
391 detection algorithm after flattening the RCF (for other layouts, see **EDF1**). Fifteen out of the sixteen
392 clusters are comprise a single plant species, while one contains two plant species (*Geranium molle*
393 and *Lavatera maritima*). Animals/fungi are associated with groups of plants to form a consortium to
394 deliver the functionality of the ecosystem.



395

396 **Figure 3: Nestedness in The MultiFunctional Ecological Network of the Na Redona dataset.** (a) 397 Illustrative cartoon of how the MultiFunctional Ecological Network \mathbf{P} whose entries are the

398 participation strengths P^a_i is computed: for plant species i , two individuals have been e.g. pollinated
 399 and participated in herbivory function (see Methods). (b) Concrete matrix Φ obtained for the Na
 400 Redona dataset, showing a stylised nested structure, which suggests that (i) plant species rank in a
 401 generalist-specialist dimension (in terms of how many functions and how strongly they participate
 402 in) and that (ii) functions rank in a generalist-specialist dimension (in terms of how many species and
 403 how intensely are involved in a given function). (c) The MultiFunctional Ecological Network of the Na
 404 Redona dataset, visualised as a bipartite (resource-function) network. (d-e) Basic generalist-
 405 specialist function rankings of functions (d) and plant species (e). By evaluating the strength
 406 contribution of nodes within each function relative to the overall strength of all nodes, we were able
 407 to determine the relative importance of each species and function within the network (see Methods).
 408
 409

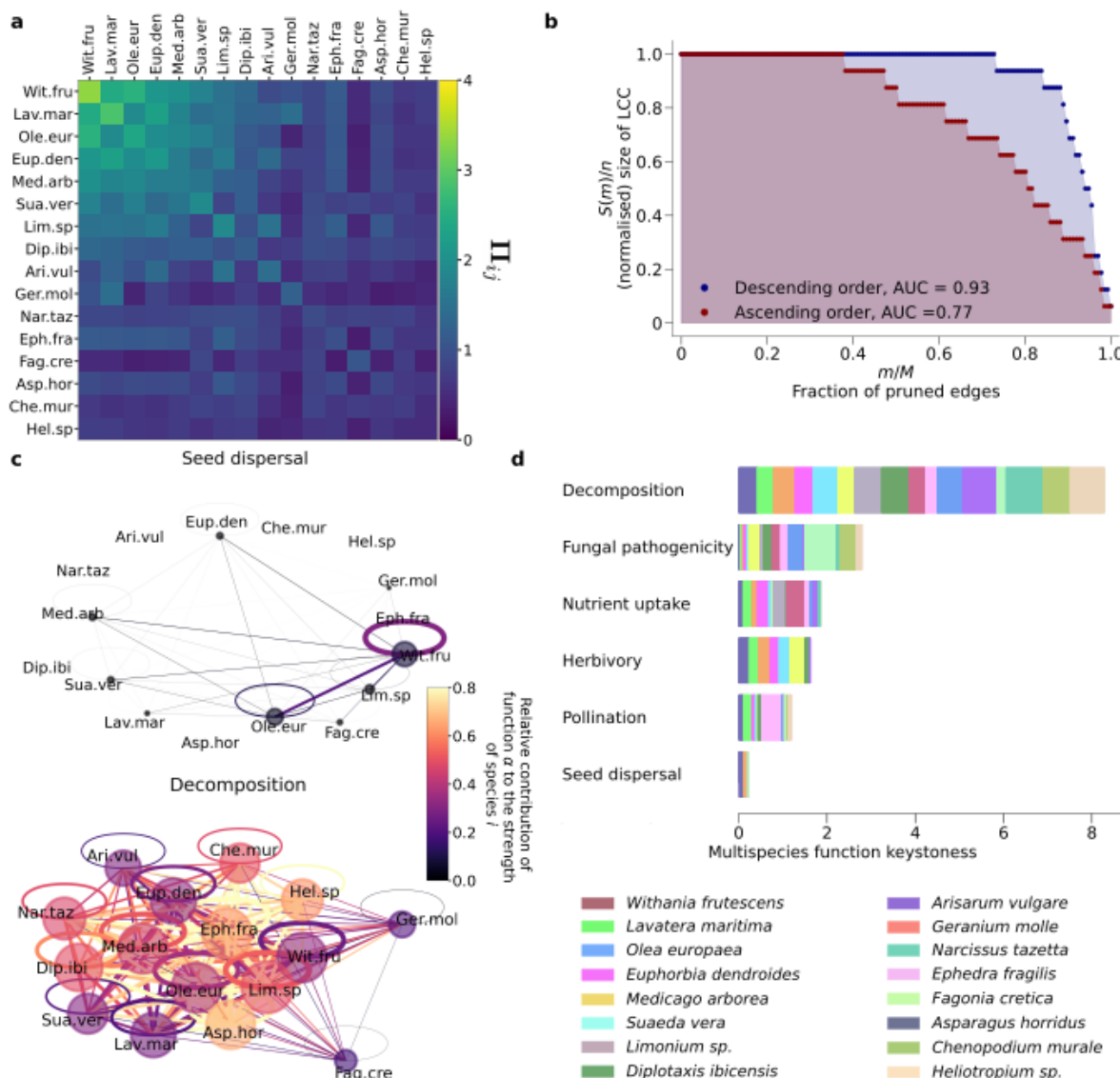


410

411 **Figure 4: Phytocentric embedding: function-function networks and multifunctional species**
 412 **keystone**. (a) Function-function network's weighted adjacency matrix Φ for the Na Redona
 413 dataset. (b) Pruning analysis of Φ , plotting $S(m)/n$, the (normalised) size of the largest connected
 414 component of the pruned Φ as a function of the fraction of deleted edges m/M , for two pruning
 415 strategies (removing edges in decreasing (blue) or increasing (red) order of link weights,
 416 respectively). The Area Under the Curve (AUC) is a measure of the network's robustness to pruning.

417 showing that it is overall robust (large AUC values), but more sensible to deletion of links with lower
 418 weight (weaker ties) as this pruning strategy results in a lower AUC. (c) Two examples of conditioned
 419 function-function networks $\Phi|_i$ computed by conditioning on the plant species *Withania frutescens*
 420 (bottom) and *Heliotropium sp* (top), showing two cases of plant species with very different
 421 multifunctional roles in the ecosystem. Node colours represents each species' relative contribution to
 422 the total strength of each function. For a species i , we obtain its contribution to function α relative to
 423 that of all species by summing the edge weights (strength) of node i in conditioned function-function
 424 network Φ relative to that of all species (function-function matrix Φ), which we call multifunctional
 425 participation index. Similarly, the colour of the edges quantify the weight relative to that of all species
 426 along the connections. (d) Multifunctional species ranking based on enriched metadata of the
 427 conditioned function-function networks. In order to rank species, we use the participation indices to
 428 obtain its keystone vector (see the text and Methods), which is shown in the figure, colour-coded to
 429 distinguish contributions from different functions.

430



431

432 **Figure 5: Function-centric embedding: plant-plant networks and multispecies function**
 433 **keystone. (a) Plant-plant network's weighted adjacency matrix $\mathbf{\Pi}_{\mathbf{II}}$ for the Na Redona dataset. (b)**

434 *Pruning analysis of Π , performed as in Fig. 4b, finding qualitatively similar results as for the*
435 *equivalent analysis on Φ although with a more emphatic role of weak ties. (c) Two examples of*
436 *conditioned plant-plant networks $\Pi|\alpha$ computed by conditioning on the functions decomposition (top)*
437 *and seed-dispersal (bottom), showing two ecological functions with very different roles as species*
438 *assemblers. (d) Multispecies function ranking based on enriched metadata of the conditioned plant-*
439 *plant networks (see text and Methods). In the panel, for each function we plot its keystone vector*
440 *(see Methods), colour-coded to distinguish contributions from different species.*

441

442 Methods

443 **Study site and field sampling.** The fieldwork was carried out on Na Redona ($39^{\circ}10'5''$ N, $2^{\circ}58'35''$
444 E), an islet of approximately 11 ha and 56 m high in the Cabrera Archipelago National Park (Balearic
445 Islands, Western Mediterranean Sea). Its primary habitat is Mediterranean shrubland with a relatively
446 rich plant species diversity (ca. 108).

447 In two contrasting seasons, a team of five people visited the islet for five consecutive days at the peak
448 of flowering (April/May) and at the peak of fruiting (October/November), to sample the different
449 types of interactions between plants and (1) pollinators, (2) herbivores, (3) seed dispersers, and root-
450 colonising (4) saprotrophic, (5) symbiotic, and (6) pathogenic fungi. In each sampling season, six
451 transects (100 m long x 10 m wide and separated from each other by at least 100 m) were established
452 to cover the main microhabitats and the entire altitudinal gradient of the island. In such transects, we
453 assessed plant abundance (number of individuals) and vegetation cover (m^2) of each plant species, and
454 we recorded all species interactions except the seed-dispersal ones (see below).

455 Plant-fungi interactions were sampled by collecting the roots of five individuals of each plant species
456 along the transects. Dry-cleaned roots were immediately preserved in silica gel until processing for
457 DNA extraction. Then, PCR amplification was performed using fungal-targeted ITS1 primers ITS1f-
458 ITS2^{57,58}. PCR products were cleaned, quantified, and sequenced at an equimolar concentration
459 (Illumina sequencing using 2×350 bp MiSeq) at GENYO (University of Granada, Spain). Reads were
460 filtered and processed using QIIME 2 pipeline⁵⁹, and assigned to fungal ASV (amplicon sequence

461 variants) using DADA2⁶⁰. Taxonomy and functional groups were determined using the UNITE
462 database⁶¹ and FUNGuild⁶².

463 To sample plant-pollinator interactions, we conducted censuses (of 10 min of duration, and at
464 different times of the day) consisting of direct observations on each plant individual. Each species was
465 observed for at least one hour during the sampling season, although the total time depended on flower
466 availability (mean = 2 h, total sampling effort across species = 29 h). In each census, we recorded any
467 animal (i.e. insects, lizards, or/and birds) that contacted the reproductive parts of the flowers. Insect
468 species were photographed and identified using the reference collection available at IMEDEA. When
469 unknown, they were captured and later identified by an entomologist, to the species level when
470 possible or to the morphospecies level otherwise. Additionally, we captured 30 lizards using a noose
471 on the tip, and 26 land birds using mist nets, being the latter not very abundant and difficult to catch
472 since the islet is dominated by open vegetation or/and shrublands. We sampled the potential pollen
473 carried by each lizard and bird by swabbing a cube (approx. 3mm³) of fuchsine-stained glycerine jelly
474 on their snout and beak and peri-mandibular feathers, respectively. The gelatine cube was then placed
475 on a microscope slide, melted, and covered with a slip. The entire slide area was inspected under a
476 light microscope to identify and count all pollen grains to species level using a pollen reference
477 collection available at IMEDEA. Evidence of flower visitation was considered if more than six pollen
478 grains of a given plant species were detected in the sample. Each captured individual was considered a
479 sampling unit.

480 Plant-herbivore interactions were evaluated in five individuals of each plant species, browsing the
481 isolated branches and recording all arthropods found feeding on plant tissues. Unknown herbivorous
482 species were captured and later identified by an entomologist, to the species level when possible or to
483 the morphospecies level otherwise.

484 Finally, to sample plant-seed disperser interactions, we collected droppings and pellets of gulls (236),
485 droppings of passerines (21), and lizards (375), and anthill material (4). We identified all taxa to plant
486 species level or morphospecies under a stereomicroscope, by comparing the seeds with a reference
487 seed collection also available at IMEDEA.

488

489 ***Estimation of the weights in the RCF tensor.*** Taking advantage of the simplicity of a small
490 island, we apply the developed framework by focusing on six layers of complexity corresponding to
491 six ecological functions: pollination, herbivory, seed-dispersal, decomposition of organic matter,
492 nutrient uptake (mycorrhizas) and fungal pathogenicity. Saprotrrophic fungi are the primary agents of
493 plant litter decomposition, thus, key regulators of nutrient cycling. Mycorrhizas play a key role in
494 terrestrial ecosystems as they regulate nutrient and carbon cycles, influencing soil structure and
495 ecosystem multifunctionality. Up to 80% of plant N and P is provided by mycorrhizal fungi and many
496 plant species depend on these symbionts for growth and survival. Fungal pathogenicity is not a
497 standard ecological function per se but can impact ecological functions and processes through its
498 effects on population dynamics, biodiversity, trophic interactions, nutrient cycling, succession, and
499 coevolution. Understanding the interactions between fungal pathogens and their is indeed important
500 for comprehending and managing the ecological consequences of these diseases^{68,69}.

501 Our common species in six layers are plants ('resources'), and we study their interactions with
502 'consumers': (1) pollinators, (2) herbivores, (3) seed dispersers, (4) saprophytic, (5) symbiotic and (6)
503 pathogenic fungi. We assume a one-to-one map from interaction type to function, i.e. every time an
504 interaction is recorded, the type of function it belongs to is also annotated -leaving no room for
505 ambiguity- regardless of the inherent interaction strength (e.g. the time elapsed in the interaction), so
506 the effective interaction strength is given through their frequency in the data. We acknowledge the
507 evidence to support the crucial role of inherently-weak interactions in ecology, as they can act as both
508 stabilizing factors and drivers of unstable dynamics^{63,64}. Our choice does not account for the
509 variability in inherent interaction strength, and a general method is needed to explore the robustness
510 of the mapping. This is highlighted in the literature on interaction strengths in food webs, which
511 emphasises the need for clarity in terminology and definition, as well as exploring new ways to
512 estimate biologically reasonable model coefficients from empirical data⁶⁵.

513 The strength of an interaction between plant species i , and animal species x at function α (i.e. at any
514 given ecological function), was calculated as:

515
$$f_{ix}^\alpha = \frac{m_{ix}^\alpha}{n_i}$$

516 where m_{ix}^α is the number of individuals of plant i on which an animal species x was detected along
517 function α , and n_i is the number of individuals of plant species i sampled. Plant–fungus interactions
518 were quantified as the proportion of different taxa ASV reads per plant species⁶⁶. For illustration, if
519 say a total of $n_i = 20$ samples of the plant species i were monitored, and 12 of them were observed
520 being pollinated by a single animal species whereas 10 of them were observed being dispersed (7 by
521 animal species 1 and 3 by animal species 2), then the associated probabilities f_{ix}^α would be 12/20,
522 7/20, and 3/20 respectively (observe that these don't add up to one: events are independent and thus
523 probabilities are only normalised in terms of an event and its complementary).
524 For example, in the case of the pollination layer, the weights of the interaction measure the fraction of
525 plants of a given species that has been observed being pollinated, in other words, the probability that a
526 random plant of species i is being pollinated.

527 **Resource-Consumer-Function tensor (RCF) visualisation.** The specific visualisation of the
528 RCF tensor presented in **Fig. 2**, containing plant species and the weight of interactions with
529 animal/fungus species, was obtained using Netgraph, a freely available library implemented in Python
530 (<https://github.com/paulbrodersen/netgraph>, last accessed: March 10, 2023). This layout also
531 incorporates a study of the mesoscale organisation of the RCF while considering the network as a
532 single-layer one. For that purpose, we used Infomap, a network clustering algorithm based on the Map
533 Equation freely available at (<https://github.com/mapequation/infomap.git>, last accessed: March 10,
534 2023). The same clusters were also found using an alternative method (Louvain community detection
535 algorithm). Generally, a plant species interacts with an animal/fungi species through a single
536 ecological function. By projecting the tensor/multigraph onto a single layer, we focus the community
537 detection algorithm's attention on the plant-animal/fungi interactions. This allowed us to visualise 15
538 clusters, which broadly group the plant-animal/fungi pairs with the strongest interactions. We used
539 different colours to identify each type of interaction and its associated animal/fungi species. For other
540 visualisations, including Infomap enriched with multilayer properties, see **EDF2**.

541 Within our data, only 3 interactions between a plant species i and an animal/fungi x were
542 catalogued as belonging to two different ecological functions. This happens, for example, when an
543 insect exhibits herbivory during its larval stage and pollination during its adult stage. These
544 interactions are represented as multilinks in the RCF, and are visualised with corresponding colours in
545 the network without overlapping. Colours are assigned to the animal/fungi nodes based on one of the
546 interactions, with a border of the colour corresponding to the other interaction.

547

548 ***Estimation of edge weights P^{α_i} in MFEN.*** To contract animals in the RCF tensor and build the
549 MFEN, we follow a simple logical manipulation of probabilities. By construction, in the RCF the
550 weight $f^{\alpha_{ix}}$ is the probability of finding a specific resource i and a specific animal/fungus x interacting
551 via a specific function α , thus $1-f^{\alpha_{ix}}$ (the negation) is the probability of *not* finding [a specific resource
552 i and a specific animal/fungus x interacting via a specific function α]. Assuming independence of
553 events, the probability of not finding a specific resource i and *any* animal/fungus x interacting via a
554 specific function α is, consequently, $\Pi_x (1-f^{\alpha_{ix}})$. We finally negate this again, so the probability of
555 finding a specific resource i and *any* animal/fungus x interacting via a specific function α is $1-\Pi_x (1-$
556 $f^{\alpha_{ix}})$. This probability is independent of x , it just describes the probability of a resource i effectively
557 interacting via a function α , i.e. the probability that a plant species i participates in a function α . We
558 call this the participation strength P^{α_i} .

559

560 ***Generalist-Specialist ranking.*** The ranking of generalist and specialist species and functions in the
561 bipartite network provides insight into the organisation and functioning of complex ecological
562 systems. In particular, we evaluated the strength contribution of nodes belonging to the function class
563 relative to the overall strength of all nodes in the class. The strength of a node is calculated by adding
564 the weights of all its edges. For a given function α , the strength of the function is obtained as $s^{\alpha} =$
565 $\sum_i P^{\alpha_i}$. Then, the overall strength of the function class can be calculated by summing the strengths of
566 all the individual functions, which can be expressed as $\sum_{\alpha} s^{\alpha}$.

567 Analogously, plant species' class nodes are also ranked based on their strength contribution
568 relative to the overall strength of the species in the bipartite network. The strength of a plant species i
569 is obtained as $s_i = \sum_{\alpha} P^{\alpha}_i$. Then, the overall strength of a species class can be calculated by adding
570 up the strengths of all individual species $\sum_i s_i$. Note that to classify species as ecological function-
571 generalists or function-specialists, both the number of functions in which they participate as well as
572 the strength of their participation must be considered³⁷.

573 **Φ and Π as similarity matrices.** Let us consider **Φ** first. Mathematically, it is an 6 x 6 matrix as we
574 have 6 different ecological functions displayed by the ecosystem. Each function-node α is enriched by
575 a vector $\mathbf{v}_{\alpha} = (P^{\alpha}_1, P^{\alpha}_2, \dots, P^{\alpha}_{16})$, where \mathbf{v}_{α} accounts for the way in which function α interacts with
576 each plant species. Accordingly, weights of the function-function network are given in terms of the
577 scalar product $\Phi^{\alpha\beta} = \mathbf{v}_{\alpha} \cdot \mathbf{v}_{\beta}$. Since a scalar product can be interpreted as a similarity measure
578 (correlation) between two vectors (with two ingredients: their magnitude and the angle between
579 them), this simple mathematical observation indicates that $\Phi^{\alpha\beta}$ accounts for how similar two functions
580 are, based on (i) how large or small is their participation strength across plants (vector magnitude),
581 and (ii) how systematically mismatched (anticorrelated) is this pattern across plants (angle between
582 vectors), i.e., it is function-to-function similarity measure emerging in a plant-feature embedding. The
583 same can be said about **Π**: under this geometrical interpretation, Π_{ij} quantifies how similar plants i
584 and j are, based on how similar their interaction patterns across functions are, i.e. it displays plant-to-
585 plant similarities in a function-feature embedding.

586 **Pruning and robustness analysis.** Starting from a weighted network, we order edge weights and
587 proceed to prune the network in either ascending or descending order of edge weights. After pruning
588 $m=1,2,\dots$ edges, we compute the size (number of nodes) of the largest connected component of the
589 network, obtaining a curve $S(m)$. $S(m)$ is a monotonically decreasing curve, whose profile is indicative
590 of the hierarchical structure of the network, and the area under this curve (AUC) determines the
591 response of the network to the perturbation, where higher values of AUC mean that the network is
592 more robust to a specific pruning strategy. To properly compare AUCs for different networks, AUC is
593 computed by normalizing $S(m)$ over the total number of nodes N , and m is normalised by dividing it

594 over the total number of edges M . We compare ascending and descending pruning strategies by
595 computing the enclosed area between the two curves, i.e. the difference between both AUCs, using a
596 quadrature rule.

597 **Multifunctional participation index and associated kestoeness.** The importance of resource i in
598 connecting ecological functions is calculated with the multifunctional participation index (MPI)⁶⁷. Let
599 the strength of function α in resource i is $s^{\alpha}_i = P^{\alpha}_i \sum_{\beta} P^{\beta}_i$ and the total connectivity of all plant
600 species (all conditioned function-function networks) through the same ecological function be $o^{\alpha} =$
601 $\sum_{i=1}^M s^{\alpha}_i$. The MPI of plant species i and function α is obtained as $\text{MPI}(i, \alpha) = s^{\alpha}_i / o^{\alpha}$. The resulting
602 kestoeness vector of plant species i is composed of the 6 MPIs, one for each function (each of these
603 MPI is colour-coded in **Fig. 4d**). The L₁-norm of such vector (i.e. the sum of all entries) allows us to
604 rank species accordingly (**Fig. 4d**). The same methodology is reproduced in the function-centric case
605 by using the change of variable $\alpha \rightarrow i$. In this way, we can compute a multispecies participation index
606 $\text{mPI}(\alpha, i) = P^{\alpha}_i \sum_{\beta} P^{\beta}_i / \sum_{\beta} \sum_i P^{\beta}_i P^{\alpha}_i$. The resulting kestoeness vector of function α is composed of
607 the 16 respective MPIs, one for each plant species (each of these mPI is colour-coded in **Fig. 5d**). The
608 L1-norm of such vector (i.e. the sum of all entries) allows us to rank functions accordingly (**Fig. 5d**).

609
610 **Acknowledgements** We thank Xavier Canyelles that identified all insects; José Antonio Morillo that
611 contributed to the bioinformatic analysis of plant-fungi interactions, Aarón González-Castro and Juan
612 Pedro González-Varo for their help in the field, and Araceli Guillem Bosch for her help in the
613 laboratory processing of pollen samples. M.C.B., L.L., and V.M.E. acknowledge funding from the
614 Spanish Research Agency (MCIN/AEI/10.13039/501100011033) via project MISLAND (PID2020-
615 114324GB-C22), the María de Maeztu project CEX2021-001164-M and project DYNDEEP
616 (EUR2021-122007). S.H.P and A.T. acknowledge funding by MCIN/AEI/10.13039/501100011033
617 (CGL2017-88122-P, PID2020-114324GB-C21) and the María de Maeztu project CEX2021- 001198-
618 M. The study is also framed within project 101054177 *IslandLife* funded by ERC AdG to A.T. I.D is

619 supported by a Marie Curie Postdoctoral Fellowship (HORIZON-TMA-MSCA-101068643). R.H.
620 was funded by the Portuguese Foundation for Science and Technology (UID/BIA/04004/2020).

621 **Code availability statement** All the necessary codes will be available upon publication in a GitHub
622 repository.

623 **Data availability statement** Data will be available upon publication in a GitHub repository.

624 **Author contributions** A.T., M.N., R.H., S.H-P. and S.R-E conceived and designed the research to
625 build the multilayer network and gathered data in the field. S.H-P. led the data curation after all taxa
626 were identified and built the multilayer network. S.R-E did the classification of fungi into the three
627 functional groups. L.L. and V.M.E. conceptualised and lead the mathematical modelling. M.C-B.
628 contributed to mathematical modelling, performed all the network analysis, data analysis and
629 simulations and generated all the figures. S.H-P, M.C-B, L.L, A.T., I.D., C.M. and V.M.E discussed
630 results. L.L., M.C-B and V.M.E. wrote the first draft, and all authors contributed to write and revise
631 the final draft.

632 **Competing interest declaration** The authors declare no competing interests.

633 **References**

- 634 1. Knight, T. M., McCoy, M. W., Chase, J. M., McCoy, K. A. & Holt, R. D. Trophic cascades across
635 ecosystems. *Nature* **437**, 880–883 (2005).
- 636 2. Keith, D. A. *et al.* A function-based typology for Earth’s ecosystems. *Nature* **610**, 513–518 (2022).
- 637 3. Kaiser-Bunbury, C. N. *et al.* Ecosystem restoration strengthens pollination network resilience and
638 function. *Nature* **542**, 223–227 (2017).
- 639 4. Suweis, S., Simini, F., Banavar, J. R. & Maritan, A. Emergence of structural and dynamical properties
640 of ecological mutualistic networks. *Nature* **500**, 449–452 (2013).
- 641 5. Fricke, E. C. & Svenning, J.-C. Accelerating homogenization of the global plant–frugivore meta-
642 network. *Nature* **585**, 74–78 (2020).
- 643 6. Manning, P. *et al.* Redefining ecosystem multifunctionality. *Nature Ecology & Evolution* **2**, 427–436
644 (2018).
- 645 7. Hector, A. & Bagchi, R. Biodiversity and ecosystem multifunctionality. *Nature* **448**, 188–190 (2007).
- 646 8. Wu, D., Xu, C., Wang, S., Zhang, L. & Kortsch, S. Why are biodiversity—ecosystem functioning
647 relationships so elusive? Trophic interactions may amplify ecosystem function variability. *Journal of
648 Animal Ecology* **92**, 367–376 (2023).
- 649 9. Marzidovšek, M., Podpečan, V., Conti, E., Debeljak, M. & Mulder, C. BEFANA: A tool for
650 biodiversity-ecosystem functioning assessment by network analysis. *Ecological Modelling* **471**,
651 110065 (2022).
- 652 10. Mori, A. S., Isbell, F. & Cadotte, M. W. Assessing the importance of species and their assemblages for
653 the biodiversity-ecosystem multifunctionality relationship. *Ecology* e4104 (2023).

654 11. Yodzis, P. The indeterminacy of ecological interactions as perceived through perturbation
655 experiments. *Ecology* **69**, 508–515 (1988).

656 12. Wootton, J. T. The nature and consequences of indirect effects in ecological communities. *Annual
657 Review of Ecology and Systematics* **25**, 443–466 (1994).

658 13. Guimaraes Jr, P. R., Pires, M. M., Jordano, P., Bascompte, J. & Thompson, J. N. Indirect effects drive
659 coevolution in mutualistic networks. *Nature* **550**, 511–514 (2017).

660 14. Eklöf, A. *et al.* The dimensionality of ecological networks. *Ecology Letters* **16**, 577–583 (2013).

661 15. Dehling, D. M. & Stouffer, D. B. Bringing the Eltonian niche into functional diversity. *Oikos* **127**,
662 1711–1723 (2018).

663 16. Anderson, P. W. More is different: broken symmetry and the nature of the hierarchical structure of
664 science. *Science* **177**, 393–396 (1972).

665 17. Brophy, C. *et al.* Biodiversity and ecosystem function: making sense of numerous species interactions
666 in multi-species communities. *Ecology* **98**, 1771–1778 (2017).

667 18. Hines, J. *et al.* Chapter Four - Towards an Integration of Biodiversity–Ecosystem Functioning and
668 Food Web Theory to Evaluate Relationships between Multiple Ecosystem Services. *Advances in
669 Ecological Research* vol. 53 161–199 (2015).

670 19. Bascompte, J. Networks in ecology. *Basic and applied ecology* **8**, 485–490 (2007).

671 20. Latora, V., Nicosia, V. & Russo, G. *Complex networks: principles, methods and applications*.
672 (Cambridge University Press, 2017).

673 21. De Domenico, M. *et al.* Mathematical formulation of multilayer networks. *Physical Review X* **3**,
674 041022 (2013).

675 22. Bianconi, G. *Multilayer networks: structure and function*. (Oxford university press, 2018).

676 23. Pilosof, S., Porter, M. A., Pascual, M. & Kéfi, S. The multilayer nature of ecological networks. *Nature
677 Ecology & Evolution* **1**, 0101 (2017).

678 24. Hutchinson, M. C. *et al.* Seeing the forest for the trees: Putting multilayer networks to work for
679 community ecology. *Functional Ecology* **33**, 206–217 (2019).

680 25. Seibold, S., Cadotte, M. W., MacIvor, J. S., Thorn, S. & Müller, J. The necessity of multitrophic
681 approaches in community ecology. *Trends in Ecology & Evolution* **33**, 754–764 (2018).

682 26. Faisal, A., Dondelinger, F., Husmeier, D. & Beale, C. M. Inferring species interaction networks from
683 species abundance data: A comparative evaluation of various statistical and machine learning
684 methods. *Ecological Informatics* **5**, 451–464 (2010).

685 27. Morueta-Holme, N. *et al.* A network approach for inferring species associations from co-occurrence
686 data. *Ecography* **39**, 1139–1150 (2016).

687 28. Siwicka, E., Gladstone-Gallagher, R., Hewitt, J. E. & Thrush, S. F. Beyond the single index:
688 Investigating ecological mechanisms underpinning ecosystem multifunctionality with network
689 analysis. *Ecology and Evolution* **11**, 12401–12412 (2021).

690 29. Maureaud, A., Andersen, K. H., Zhang, L. & Lindegren, M. Trait-based food web model reveals the
691 underlying mechanisms of biodiversity–ecosystem functioning relationships. *Journal of Animal
692 Ecology* **89**, 1497–1510 (2020).

693 30. Bascompte, J. Disentangling the web of life. *Science* **325**, 416–419 (2009).

694 31. Murdoch, W. W., Briggs, C. J. & Nisbet, R. M. Consumer-resource dynamics (MPB-36). in
695 *Consumer-Resource Dynamics (MPB-36)* (Princeton University Press, 2013).

696 32. Daly, H. E. & Farley, J. *Ecological economics: principles and applications*. (Island press, 2011).

697 33. Mariani, M. S., Ren, Z.-M., Bascompte, J. & Tessone, C. J. Nestedness in complex networks:
698 observation, emergence, and implications. *Physics Reports* **813**, 1–90 (2019).

699 34. Mack, K. M., Eppinga, M. B. & Bever, J. D. Plant-soil feedbacks promote coexistence and resilience
700 in multi-species communities. *PLoS One* **14**, e0211572 (2019).

701 35. Desurmont, G. A. *et al.* Alien interference: disruption of infochemical networks by invasive insect
702 herbivores. *Plant, Cell & Environment* **37**, 1854–1865 (2014).

703 36. Yen, J. D. *et al.* Linking structure and function in food webs: maximization of different ecological
704 functions generates distinct food web structures. *Journal of Animal Ecology* **85**, 537–547 (2016).

705 37. Flynn, D. F. *et al.* Loss of functional diversity under land use intensification across multiple taxa.
706 *Ecology Letters* **12**, 22–33 (2009).

707 38. Granovetter, M. The strength of weak ties: A network theory revisited. *Sociological Theory* 201–233
708 (1983).

709 39. Agliari, E., Cioli, C. & Guadagnini, E. Percolation on correlated random networks. *Physical Review E*
710 **84**, 031120 (2011).

711 40. Valdano, E. & Arenas, A. Exact Rank Reduction of Network Models. *Physical Review X* **9**, 031050
712 (2019).

713 41. Caldarelli, G., Capocci, A., De Los Rios, P. & Munoz, M. A. Scale-free networks from varying vertex
714 intrinsic fitness. *Physical Review Letters* **89**, 258702 (2002).

715 42. Boguná, M. & Pastor-Satorras, R. Class of correlated random networks with hidden variables.
716 *Physical Review E* **68**, 036112 (2003).

717 43. Timóteo, S. *et al.* Tripartite networks show that keystone species can multitask. *Functional Ecology*
718 **37**, 274–286 (2023).

719 44. Soliveres, S. *et al.* Biodiversity at multiple trophic levels is needed for ecosystem multifunctionality.
720 *Nature* **536**, 456–459 (2016).

721 45. Byrnes, J. E., Roger, F. & Bagchi, R. Understandable multifunctionality measures using Hill numbers.
722 *Oikos* **2023**, e09402 (2023).

723 46. Onnela, J.-P. *et al.* Structure and tie strengths in mobile communication networks. *Proceedings of the
724 National Academy of Sciences* **104**, 7332–7336 (2007).

725 47. Mello, M. A. R. *et al.* Keystone species in seed dispersal networks are mainly determined by dietary
726 specialization. *Oikos* **124**, 1031–1039 (2015).

727 48. Alberch, P. From genes to phenotype: dynamical systems and evolvability. *Genetica* **84**, 5–11 (1991).

728 49. Hidalgo, C. A., Klinger, B., Barabási, A.-L. & Hausmann, R. The product space conditions the
729 development of nations. *Science* **317**, 482–487 (2007).

730 50. Iler, A. M., CaraDonna, P. J., Forrest, J. R. & Post, E. Demographic consequences of phenological
731 shifts in response to climate change. *Annual Review of Ecology, Evolution, and Systematics* **52**, 221–
732 245 (2021).

733 51. Rogers, H. S., Donoso, I., Traveset, A. & Fricke, E. C. Cascading impacts of seed disperser loss on
734 plant communities and ecosystems. *Annual Review of Ecology, Evolution, and Systematics* **52**, 641–
735 666 (2021).

736 52. Tylianakis, J. M. & Morris, R. J. Ecological networks across environmental gradients. *Annual Review of
737 Ecology, Evolution, and Systematics* **48**, 25–48 (2017).

738 53. Hervías-Parejo, S. *et al.* Species functional traits and abundance as drivers of multiplex ecological
739 networks: first empirical quantification of inter-layer edge weights. *Proc. R. Soc. B.* **287**, 20202127
740 (2020).

741 54. Antqueira, P. A. P., Petchey, O. L. & Romero, G. Q. Warming and top predator loss drive ecosystem
742 multifunctionality. *Ecology Letters* **21**, 72–82 (2018).

743 55. Moi, D. A. *et al.* Human pressure drives biodiversity–multifunctionality relationships in large
744 Neotropical wetlands. *Nature Ecology & Evolution* **6**, 1279–1289 (2022).

745 56. Brauns, M. *et al.* A global synthesis of human impacts on the multifunctionality of streams and rivers.
746 *Global Change Biology* **28**, 4783–4793 (2022).

747 57. Kohout, P. *et al.* Comparison of commonly used primer sets for evaluating arbuscular mycorrhizal
748 fungal communities: is there a universal solution? *Soil Biology and Biochemistry* **68**, 482–493 (2014).

749 58. Walters, W. *et al.* Improved bacterial 16S rRNA gene (V4 and V4-5) and fungal internal transcribed
750 spacer marker gene primers for microbial community surveys. *Msystems* **1**, e00009-15 (2016).

751 59. Bolyen, E. *et al.* Reproducible, interactive, scalable and extensible microbiome data science using
752 QIIME 2. *Nature Biotechnology* **37**, 852–857 (2019).

753 60. Callahan, B. J. *et al.* DADA2: High-resolution sample inference from Illumina amplicon data. *Nature
754 Methods* **13**, 581–583 (2016).

755 61. Kõlalg, U. *et al.* UNITE: a database providing web-based methods for the molecular identification of
756 ectomycorrhizal fungi. *New Phytologist* **166**, 1063–1068 (2005).

757 62. Nguyen, N. H. *et al.* FUNGuild: an open annotation tool for parsing fungal community datasets by
758 ecological guild. *Fungal Ecology* **20**, 241–248 (2016).

759 63. McCann, K., Hastings, A. & Huxel, G. R. Weak trophic interactions and the balance of nature. *Nature*
760 **395**, 794–798 (1998).

761 64. Berlow, E. L., Navarrete, S. A., Briggs, C. J., Power, M. E. & Menge, B. A. Quantifying variation in
762 the strengths of species interactions. *Ecology* **80**, 2206–2224 (1999).

763 65. Berlow, E. L. *et al.* Simple prediction of interaction strengths in complex food webs. *Proceedings of
764 the National Academy of Sciences* **106**, 187–191 (2009).

765 66. Öpik, M., Metsis, M., Daniell, T., Zobel, M. & Moora, M. Large-scale parallel 454 sequencing reveals
766 host ecological group specificity of arbuscular mycorrhizal fungi in a boreonemoral forest. *New
767 Phytologist* **184**, 424–437 (2009).

768 67. Battiston, F., Nicosia, V. & Latora, V. Structural measures for multiplex networks. *Physical Review E*
769 **89**, 032804 (2014).

770 68. Garrido, J. L. et al. The structure and ecological function of the interactions between plants and
771 arbuscular mycorrhizal fungi through multilayer networks. *Funct. Ecol.* (2023).

772 69. Frąc, M., Hannula, S. E., Bełka, M. & Jędryczka, M. Fungal biodiversity and their role in soil
773 health. *Front. Microbiol.* 9, 707 (2018).

774

775